

# Quantum Information Processing through Nuclear Magnetic Resonance

J. D. Bulnes<sup>1</sup>, F. A. Bonk<sup>2</sup>, R. S. Sarthour<sup>1</sup>, E. R. de Azevedo<sup>2</sup>,

J. C. C. Freitas<sup>3</sup>, T. J. Bonagamba<sup>2</sup>, and I. S. Oliveira<sup>1</sup>

(1) Centro Brasileiro de Pesquisas Físicas, Rua Dr. Xavier Sigaud 150, Rio de Janeiro, RJ, 22290-180, Brazil

(2) Instituto de Física de São Carlos, Universidade de São Paulo,

Caixa Postal 369, São Carlos, 13560-970, SP, Brazil and

(3) Departamento de Física, Universidade Federal do Espírito Santo, Vitória, 22060-900, ES, Brazil

Received on 31 January, 2005

We discuss the applications of Nuclear Magnetic Resonance (NMR) to quantum information processing, focusing on the use of quadrupole nuclei for quantum computing. Various examples of experimental implementation of logic gates are given and compared to calculated NMR spectra and their respective density matrices. The technique of *Quantum State Tomography* for quadrupole nuclei is briefly described, and examples of measured density matrices in a two-qubit  $I = 3/2$  spin system are shown. Experimental results of density matrices representing pseudo-Bell states are given, and an analysis of the entropy of these states is made. Considering an NMR experiment as a depolarization quantum channel we calculate the entanglement fidelity and discuss the criteria for entanglement in liquid state NMR quantum information. A brief discussion on the perspectives for NMR quantum computing is presented at the end.

## I. INTRODUCTION

Pulsed Nuclear Magnetic Resonance (NMR) has a very long history of success in science and technology. The technique has been broadly used in Chemistry, Biology, Physics and Medicine [1–4] and, more recently, it has found a new exciting application: quantum information processing [5]. Since the discovery of the so-called *pseudo-pure states* by Gershenfeld and Chuang in 1997 [6] and Cory et al. [7], there has been a rapidly growing interest in NMR quantum computing, and virtually all quantum logic gates and algorithms have been demonstrated through NMR [8–10]. Very recent experimental advances in NMR promise to bring further interest into this technique for quantum information processing [11, 12].

Quantum computation, as much the same as classical computation, is built upon a finite set of quantum logic gates [5], and any technique aimed to implement quantum algorithms must be able to implement this universal set of operations. However, such ability seems to be a necessary but not sufficient condition to quantum computation. Indeed, although NMR is recognized to correctly produce the unitary transformations which implement the universal set of quantum logic gates, Braunstein et al. [13, 14] pointed out that this is no guarantee that the expected effect will occur in the system. Here the concern is *entanglement*.

## II. ENTANGLEMENT

Consider a two-partite quantum system, with nuclear spins  $I_A = I_B = 1/2$ , in a spin singlet state [15]:

$$|\Psi\rangle = \frac{1}{\sqrt{2}}(|+1/2\rangle_A \otimes |-1/2\rangle_B - |-1/2\rangle_A \otimes |+1/2\rangle_B) \quad (1)$$

This state does not depend on the relative distance between the spins and, quantum mechanics tells us that, as long as the system remains isolated from the environment, the state will

remain unchanged. States like the above one are called *entangled*, and cannot be written as a tensor product of states of the individual components. In other words, there exist no single-particle states  $|\phi\rangle_A$  and  $|\eta\rangle_B$  such as that  $|\Psi\rangle$  could be written in the form:

$$|\Psi\rangle = |\phi\rangle_A \otimes |\eta\rangle_B \quad (2)$$

In fact, it is a simple matter to show that, whereas the combined state is a pure state, each component is in a maximally mixed state [5].

States like (1) are pure entangled, and like (2) are separable. In the language of density matrices, *strongly* separable states are those ones which can be written as  $\rho = \rho_A \otimes \rho_B$ , and *weakly* separable those ones for which  $\rho = \sum_i p_i \rho_{A,i} \otimes \rho_{B,i}$  where  $p_i$  are probabilities for the occurrence of the product state “ $i$ ”. Density matrices which cannot be written in either form are said to be entangled. It is not a simple matter to establish a general representation of entangled states, and for this reason it is important to have relatively simple criteria to characterize the degree of entanglement in a quantum system.

It is important to mention that the usual physical interpretation given to entangled states has been questioned by some authors. For instance, in Ref. [16] it is stated that: “Some authors would like to draw far-reaching philosophical conclusions [...] ‘as quantum mechanics violates realism or objective existence of phenomena’, or ‘measurement of one subsystem influences the result of the measurement of another distant subsystem which interacted in the past with the first one’. We think that these deep conclusions are premature, and it is useful to investigate explicitly many models”.

In spite of philosophical discussions about it, entanglement is possibly the main natural resource for quantum computation [5], and it has been reported in an impressive variety of NMR quantum computing experiments (for instance, [17–19]). It is present in superdense coding, in quantum teleportation, in quantum error correction protocols and in exponentially fast quantum algorithms [5]. For two qubits, there are four possible entangled states, the so-called Bell states:

$$|\Psi^\pm\rangle = \frac{|00\rangle \pm |11\rangle}{\sqrt{2}}$$

$$|\Phi^\pm\rangle = \frac{|01\rangle \pm |10\rangle}{\sqrt{2}} \quad (3)$$

Such states can easily be produced by NMR through a simple quantum circuit containing only two gates (the so-called Hadamard and CNOT gates [5]), as shown in section V of the present paper. For that, the two qubits must be first prepared in the initial state  $|00\rangle$  and then pass through the circuit. However, although bulk NMR can implement the quantum circuit for entanglement, in its present stage of development, it cannot produce pure states such as  $|00\rangle$ , but rather *pseudo-pure states* with the form:

$$\rho_\varepsilon = (1 - \varepsilon)\frac{I}{4} + \varepsilon|00\rangle\langle 00| \quad (4)$$

where  $\varepsilon \cong \mu H/k_B T \approx 10^{-5}$  for room temperature NMR, and  $I$  the  $4 \times 4$  identity matrix. Since the NMR observables are traceless quantities [20], only the second term on the right side of the above equation contribute to the detected signal. Therefore, NMR is capable of detecting signals coming from nuclei in the *same* quantum state over a maximum entropy background!

$$P_1 = \begin{pmatrix} 0.5 & 0 \\ 0 & 0.5 \end{pmatrix}; \quad P_2 = \begin{pmatrix} 0.5 & -0.5i \\ 0.5i & 0.5 \end{pmatrix}; \quad P_3 = \begin{pmatrix} 0.5 & 0.5 \\ 0.5 & 0.5 \end{pmatrix}; \quad P_4 = \begin{pmatrix} 1 & 0 \\ 0 & 0 \end{pmatrix} \quad (7)$$

and after partial transposing [21], one obtains the following eigenvalues for the resulting matrix:  $\lambda_1 = 0.249985, \lambda_2 = \lambda_3 = \lambda_4 = 0.250005$ . Since all  $\lambda$ 's are non-negative, according to Peres criterium,  $\rho_\varepsilon$  is separable, even in this example where  $\rho_1$  is a pure entangled state. Later on this paper we will argue that the analysis of Braunstein et. al. [13] was incomplete, besides showing that their established bounds for separability were not generally correct. Before that, we will also exemplify a number of quantum gates and circuit implementation through numerical examples and experimental results obtained in a two-qubit system, namely  $^{23}\text{Na}$  nuclei in a lyotropic liquid crystal, and conclude with a brief discussion about the perspectives for NMR quantum computing.

### III. QUADRUPOLAR VS SPIN-1/2 NUCLEI

The majority of NMR quantum computing experiments have been performed using spin 1/2 nuclei "(In this paper we will be concerned only to two-qubits systems.)", such as  $^1\text{H}$  and  $^{13}\text{C}$ . In these systems, each qubit is identified with a nu-

Following this reasoning, an entangled NMR state (for instance the *cat state*) can be created applying a set of unitary transformations to Eq. (2). Such state is represented by a density matrix of the form:

$$\rho_\varepsilon = (1 - \varepsilon)\frac{I}{4} + \varepsilon|\Psi^+\rangle\langle\Psi^+| \quad (5)$$

Braunstein and co-workers [13] established a lower bound for  $\varepsilon$ , below which  $\rho_\varepsilon$  is always separable. Based on their results, the authors concluded that no entanglement phenomenon has ever taken place in NMR experiments, and the experimental results reported to date could be interpreted in terms of classical correlations between spins.

In order to illustrate this point, consider the following example of entangled NMR pseudopure state:

$$\rho_\varepsilon = \frac{1 - \varepsilon}{4} \begin{pmatrix} 1 & 0 & 0 & 0 \\ 0 & 1 & 0 & 0 \\ 0 & 0 & 1 & 0 \\ 0 & 0 & 0 & 1 \end{pmatrix} + \varepsilon \begin{pmatrix} 0.5 & 0 & 0 & 0.5 \\ 0 & 0 & 0 & 0 \\ 0 & 0 & 0 & 0 \\ 0.5 & 0 & 0 & 0.5 \end{pmatrix} \quad (6)$$

and let  $\varepsilon = 2 \times 10^{-5}$ . Note that in this example  $\rho_1$  ( $\rho_\varepsilon = (1 - \varepsilon)\frac{I}{4} + \varepsilon\rho_1$ ) is a pure cat state. Let us apply the Peres criterium [21] to show that such a matrix is separable. Expanding  $\rho_\varepsilon$  in the basis of density matrix  $\{P_{i_1} \otimes P_{i_2}\}$ , defined as,

clear spin. For instance, the chloroform molecule ( $\text{CHCl}_3$ ) has two qubits, one from the carbon and the other from hydrogen nuclei. Such a system evolves under the effective hamiltonian [20]:

$$\frac{\mathcal{H}_{eff}}{\hbar} = -(\omega - \omega_C)I_z^C - (\omega - \omega_H)I_z^H + 2\pi J I_z^C I_z^H - \omega_1^C I_x^C - \omega_1^H I_x^H \quad (8)$$

where the symbols have their usual meaning [20]. The evolution is described through the unitary transformation:

$$|\psi(t)\rangle = \exp\left[-i\frac{\mathcal{H}_{eff}}{\hbar}t\right]|\psi(0)\rangle \quad (9)$$

A specific resonance can be selected by tuning the excitation field frequency (radiofrequency, RF)  $\omega$  to  $\omega_C$  or  $\omega_H$ . The control of the amplitude,  $\omega_1$ , duration and phases ( $x, y, -x, -y$ ) of the radiofrequency pulses allow any quantum logic gate to be implemented [5, 22, 23].

An alternative NMR two-qubit system is a quadrupole nucleus with  $I = 3/2$ . The effective hamiltonian for such a system is simpler than the previous one:

$$\frac{\mathcal{H}_{eff}}{\hbar} = -(\omega - \omega_0)I_z - \omega_1 I_x + \omega_Q[3I_z^2 - I^2] \quad (10)$$

Some main differences between the two systems are:

1. The number of qubits per nucleus,  $N$ , is bigger in quadrupole systems;
2. Quadrupolar splittings are usually many orders of magnitude larger than  $J$ -couplings and therefore spectral resolution is better (typically,  $\omega_Q/2\pi \approx 10 - 100$  kHz, whereas  $2\pi J/\hbar \approx 10 - 300$  Hz);
3. The free evolution of quadrupole spins goes under the propagator  $\exp(-3i\omega_Q t I_z^2)$ , whereas in the case of spins  $1/2$  it goes as  $\exp(-i2\pi J t I_{1z} I_{2z}/\hbar)$ ;
4. Phase control of individual states in a superposition is not as straightforward for quadrupole nuclei as for spin  $1/2$  systems;
5. Quadrupole relaxation is usually much faster than the spin  $1/2$  counterpart.

In the remaining of this paper we will be concerned only to quadrupole two-qubit systems.

#### IV. QUANTUM STATE TOMOGRAPHY

NMR states can be properly described using the formalism of *density matrices*,  $\rho$  [20]. For time-independent hamiltonians, under a unitary transformation,  $U$ , a density matrix evolves according to [20]:

$$\rho(t) = U(t)\rho(0)U^\dagger(t) \quad (11)$$

From  $\rho(t)$ , the NMR observables  $M^\pm = M_x \pm iM_y$  can be obtained at any instant of time from [20]:

$$M^\pm(t) = \hbar\gamma_n \text{Tr}[\rho(t)(I_x \pm iI_y)] \quad (12)$$

The Fourier Transform of the signal  $M^\pm(t)$  yields the NMR spectrum, which in the case of a  $I = 3/2$  system is composed by three lines with amplitudes  $A_1, A_2$ , and  $A_3$ , corresponding to the spin transitions  $+3/2 \rightarrow +1/2$ ,  $+1/2 \rightarrow -1/2$  and  $-1/2 \rightarrow -3/2$  (Fig. 1). In order to fully characterize the quantum state, the complete density matrix is necessary, but the trace operation in the above expression transforms an object with 16 complex entries (the density matrix of a  $I = 3/2$  spin) into a single number. Obviously information is lost in this process, but fortunately there is a way out. The technique to rebuilt  $\rho$  from measured NMR signals is called *Quantum State Tomography* and was suggested by Vogel and Risken [24], for spin  $1/2$  systems. For quadrupolar spins, the technique was first reported by Bonk et al. [25]. The deviation density matrix (labeled here as  $\rho$ ) can be considered to have the general form “( Since NMR is not sensitive to the unity

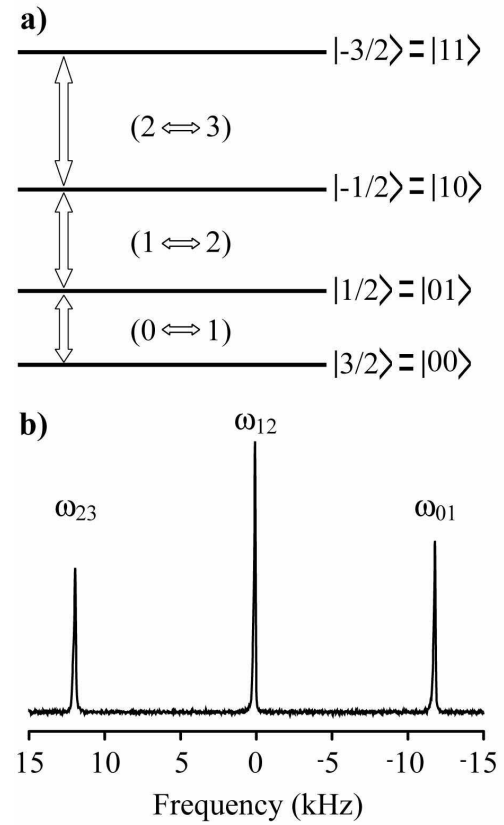


FIG. 1: (a) Nuclear Zeeman levels scheme and logical labeling for a  $I = 3/2$  spin. (b) Equilibrium NMR spectrum of  $^{23}\text{Na}$  in a lyotropic liquid crystal.

matrix of pseudo-pure states, Eq. (2), the matrix (13) must be interpreted as the *deviation matrix* of pseudo-pure states.)”

$$\rho = \begin{pmatrix} a & x_a + iy_a & x_b + iy_b & x_c + iy_c \\ x_a - iy_a & b & x_d + iy_d & x_e + iy_e \\ x_b - iy_b & x_d - iy_d & c & x_f + iy_f \\ x_c - iy_c & x_e - iy_e & x_f - iy_f & d \end{pmatrix} \quad (13)$$

The method described in [25] is based on the fact that the NMR spectra amplitudes are related only to the *diagonal* elements of  $\rho$ :

$$A_1 = \sqrt{3}(e_{11}e_{12}a - e_{12}e_{22}b - e_{23}e_{13}c - e_{13}e_{14}d)$$

$$A_2 = 2(e_{13}e_{12}a + e_{22}e_{23}b - e_{23}e_{22}c - e_{13}e_{12}d)$$

$$A_3 = \sqrt{3}(e_{13}e_{14}a + e_{13}e_{23}b + e_{12}e_{22}c - e_{11}e_{12}d) \quad (14)$$

where  $e_{ij}$  are the elements of the matrix which represent the read-out pulse [25]. The other elements are obtained applying

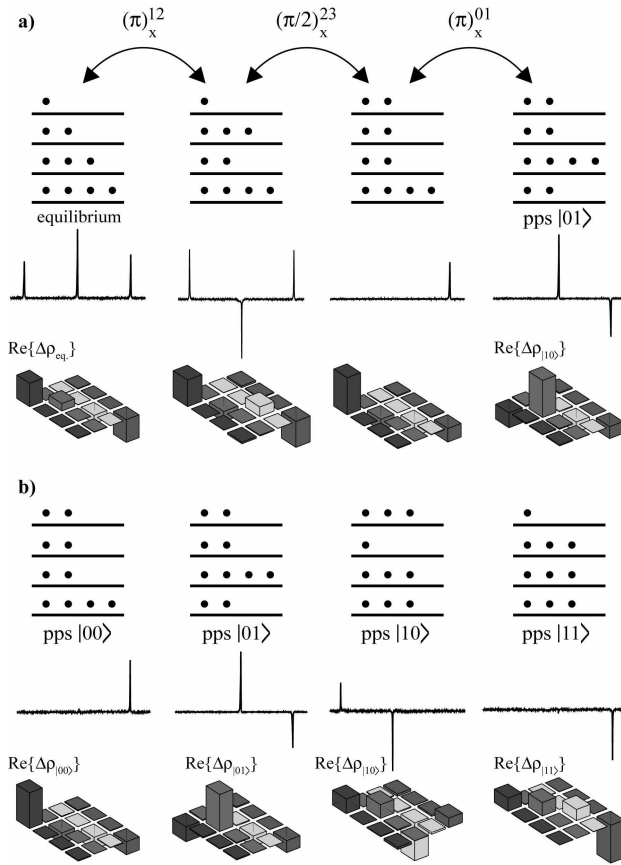


FIG. 2: Escheme representing the relative population for the energy levels, their experimental NMR spectra and respective tomographed density matrices, for (a) the steps for the creation of a pseudo pure state  $|01\rangle$  and (b) the four computational base states of  $^{23}\text{Na}$ .

pulse sequences which bring them into the main diagonal of  $\rho$ , and repeating the procedure for measuring the new diagonal elements  $d'$ ,  $b'$ ,  $c'$  and  $d'$  from the above equation. Fig. 2 shows an example of the procedure applied to the four computational base states, along with the respective NMR spectra and a scheme of the energy levels and labelling. It is important to notice that the imaginary part of  $\rho$  is negligible, and also that the amplitudes of the diagonal elements are in the correct proportions of the spins state and the levels populations.

The  $^{23}\text{Na}$  NMR experiments described in this paper were performed using a 9.4 T - VARIAN INOVA spectrometer and a home-built single-resonance probe making use of a lyotropic liquid crystal system. Gaussian shaped RF pulses with typical duration of 0.5 ms were used to perform selective saturation  $(\pi/2)$  and inversion  $(\pi)$  of populations. A non-selective hard  $\pi/20$  pulse 1.5  $\mu\text{s}$  long was applied in order to read the population differences for the three pairs of neighbor levels. Experiments were performed with a recycle delay of 500 ms. The  $^{23}\text{Na}$  NMR spectra were obtained averaging the free induction decay (FID) signal using the standard CYCLOPS scheme.

More information about the sample preparation and experimental procedures can be found in references [1], [2], [25] and [26].

## V. NMR QUANTUM LOGIC GATES

In what follows we will exemplify two of the most important quantum logic gates: the controlled-not (CNOT) and Hadamard (H) gates. CNOT (CNOT<sub>A</sub> indicates that the control qubit is the first one, whereas CNOT<sub>B</sub> indicates that the gate is controlled by the second qubit) is a two-qubit gate, whereas Hadamard acts on a single qubit. Their actions are specified by (“Here, the first qubit is the *control* qubit and the second the *target* qubit.”):

$$\begin{aligned} \text{CNOT}_A|00\rangle &= |00\rangle \\ \text{CNOT}_A|01\rangle &= |01\rangle \\ \text{CNOT}_A|10\rangle &= |11\rangle \\ \text{CNOT}_A|11\rangle &= |10\rangle \end{aligned} \quad (15)$$

and

$$\begin{aligned} H|0\rangle &= \frac{|0\rangle + |1\rangle}{\sqrt{2}} \\ H|1\rangle &= \frac{|0\rangle - |1\rangle}{\sqrt{2}} \end{aligned} \quad (16)$$

It is important to observe that, besides creating a uniform superposition of the two eigenstates of a qubit, the Hadamard gate flips the *relative phase* between the states. This property makes Hadamard a self-inverse gate:

$$H^2|0\rangle = |0\rangle \quad (17)$$

The combination of Hadamard (applied to the second qubit) and CNOT is a quantum circuit which, if applied to the initial state  $|00\rangle$ , creates entanglement:

$$\text{CNOT}_B \cdot H_B|00\rangle = \frac{|00\rangle + |11\rangle}{\sqrt{2}} \quad (18)$$

In the NMR of a  $I = 3/2$  quadrupole nucleus, these gates are generated by the following pulse sequences (“Notation:  $(\theta)_{ij}^\phi$  represents a radiofrequency pulse applied to the transition  $i \rightarrow j$ , with phase  $\phi$ , and which rotates the state by the *nutration angle*  $\theta$ . The gates subscript “A” refers to the first qubit of the pair:  $|AB\rangle$ .”) (time runs from left to right):

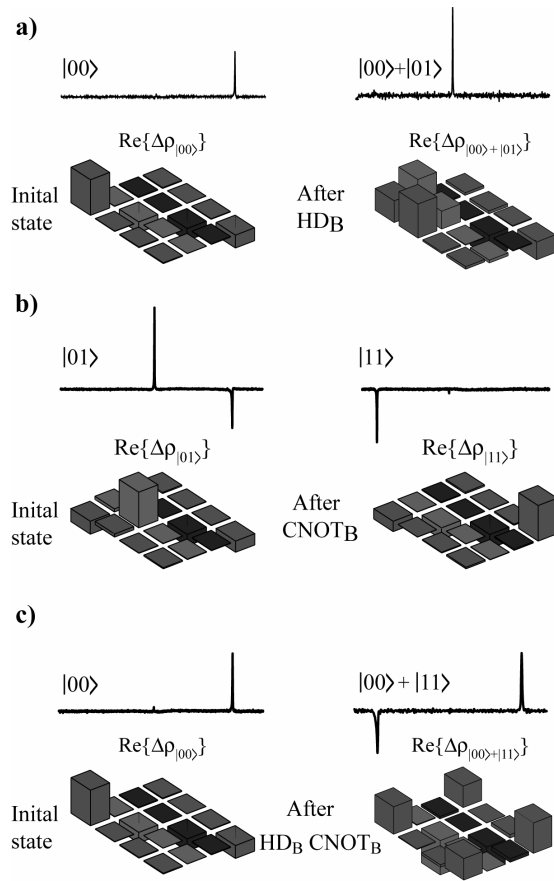


FIG. 3: Experimental NMR spectra and respective tomographed density matrices, for (a) before and after the operation  $H_B |00\rangle = \frac{1}{\sqrt{2}} [|00\rangle + |01\rangle]$  (Hadamard gate applied to the second qubit), (b)  $CNOT_B |01\rangle = |11\rangle$  (Controlled NOT - control is on the second qubit) and (c)  $CNOT_B \cdot H_B |00\rangle = \frac{1}{\sqrt{2}} [|00\rangle + |11\rangle]$ .

$$CNOT_B = (\pi)_{12}^y - (\pi)_{23}^y - (\pi)_{12}^x$$

$$H_B = (\pi/2)_{01}^y - (\pi)_{01}^x \quad (19)$$

The density matrices and corresponding NMR spectra, obtained from the experiments, are illustrated in Fig. 3. There, the initial and final states after the application of the Hadamard and CNOT logic gates, as explained in the figure. It is important to notice that the same NMR spectrum corresponds to different density matrices, as may be seen on Fig. 4. This exemplifies the reason why quantum state tomography must be done if one wishes to fully characterize the quantum state.

Figure 5 shows the evolution of the Bloch vectors of the two qubits under the action of the Hadamard gate, obtained from the relation [5]

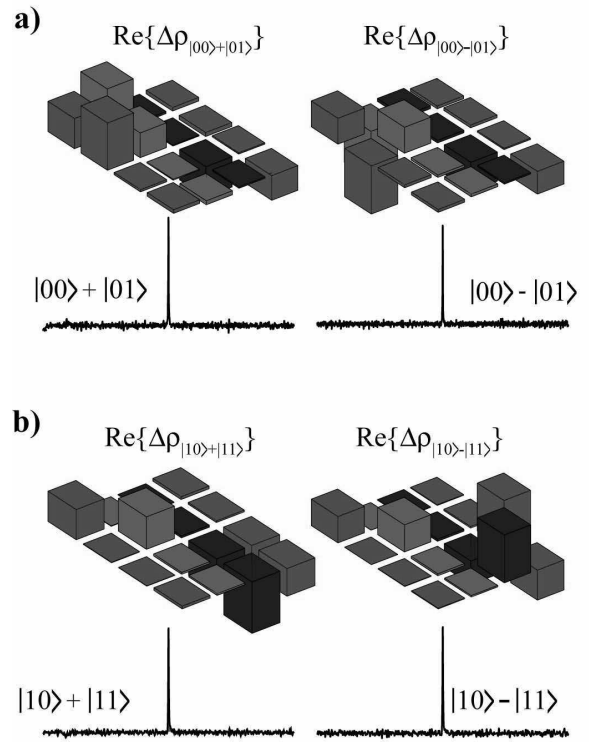


FIG. 4: Experimental NMR spectra and respective tomographed density matrices, for the four bell states, as indicated on the figure.

$$\rho = \frac{\mathbf{I} + \mathbf{r}(t) \cdot \boldsymbol{\sigma}}{2} \quad (20)$$

where  $\boldsymbol{\sigma}$  is a vector whose components are the Pauli matrices. As can be seen from the figure, the first qubit (a) does not vary as second one (b) evolves as predicted theoretically (the full line).

One important issue of NMR quantum computing which must be addressed is the relaxation. The Hamiltonian, given in equation (10), is assumed to be static, but fluctuations in time occur in both, magnetic and electric contributions. They lead to relaxation, and then to loss of coherence. Therefore, it is important to investigate relaxation in the context of NMR quantum computing. References [26] and [27] reports a spin-lattice relaxation study of various NMR quantum computing coherent states.

## VI. NMR ENTANGLEMENT

Entanglement is the main ingredient of quantum computation. But unfortunately entanglement is very difficult to be characterized by testing its non-local properties. Measurements in NMR are not projective, but ensemble averages. Long et al. [28] have proposed that an NMR state like

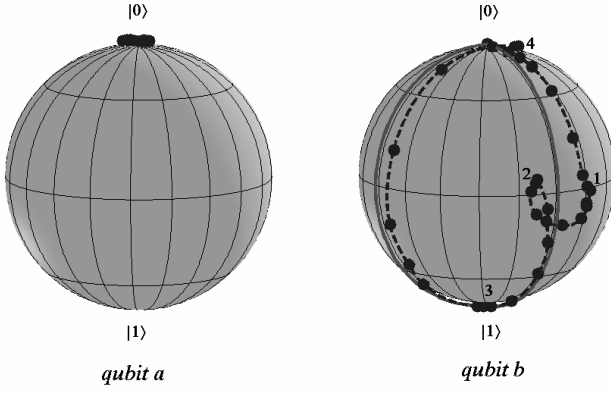


FIG. 5: The trajectory of the Bloch vector, for each individual qubit, during the evolution of the spin 3/2 quantum system, under the application of Hadamard gate twice. The points are experimental results, the dotted line is an interpolation of the data and the continuous line is a numerical simulation. Numbers indicate the end of each step (RF pulse). Each point in the figure correspond to tomographed density matrices.

$$\rho_\varepsilon = (1 - \varepsilon) \frac{I}{4} + \frac{\varepsilon}{4} (|00\rangle + |11\rangle)(\langle 00| + \langle 11|) \quad (21)$$

must be interpreted as a state in which a fraction  $\varepsilon$  of the qubits pairs are entangled in the state  $(|00\rangle + |11\rangle)/\sqrt{2}$ . Since NMR is sensitive only to the deviation density matrix (“Room temperature NMR density matrices can always be written in the form:  $\rho_\varepsilon = (1 - \varepsilon)I/d + (\varepsilon/d)\rho_1$ , where  $d$  is the dimension of the Hilbert space, and  $\rho_1$  is the so-called *deviation density matrix*.”), the detected NMR state would, according to the authors, truly reflect entanglement.

On another hand, Braunstein et. al. [13] have established bounds for  $\rho_\varepsilon$  to be entangled. The general problem is to establish the conditions for which *arbitrary* density matrices of  $N$  qubits with the form

$$\rho_\varepsilon = \frac{1}{2^N} (1 - \varepsilon)I + \varepsilon\rho_1 \quad (22)$$

can be separable. Here  $\rho_1$  represents an *arbitrary density matrix*.

Density matrices can be expanded in a basis of Pauli matrices [13]:

$$\rho = \frac{1}{2^N} c_{\alpha_1 \dots \alpha_N} \sigma_{\alpha_1} \otimes \dots \otimes \sigma_{\alpha_N} \quad (23)$$

where the coefficients  $\alpha_s$  may assume the values  $\{\alpha = 0, 1, 2, 3\}$  (being  $\sigma_0 = I$ ,  $\sigma_1 = \sigma_x$ ,  $\sigma_2 = \sigma_y$ ,  $\sigma_3 = \sigma_z$ ) and “ $s$ ” indicates the  $s$ -th qubit with the sum made over repeated indices. Normalization imposes the condition  $c_{0 \dots 0} = 1$  and the other coefficients are assumed to be in the interval  $-1 \leq c_{\alpha_1 \dots \alpha_N} \leq 1$ . Braunstein et al. [13] established that, for two qubits, taking the minimum value of the coefficients,

$c_{\alpha_1, \alpha_2} = -1$ , the bound  $\varepsilon \leq 1/15$  limits the region below which  $\rho_\varepsilon$  is separable. Generalization for arbitrary number of qubits,  $N$ , leads to  $\varepsilon \leq 1/4^N$ . On another hand, since typically  $\varepsilon \approx 10^{-5}$  in bulk NMR experiments, at room temperature, the authors conclude that not less than 13 qubits would be necessary in order to get out of the separability region, with the present NMR technology. One important observation is that in Ref. [13] (implicitly) *this bound is assumed to hold independently of  $\rho_1$* .

This bound can be made more precise if we notice that the interval taken for the coefficients  $c_\alpha$  in [13] lead to non-physical density-matrices. In what follows, we illustrate the case  $N = 2$ , for which:

$$\rho_{N=2} = \frac{1}{4} \begin{pmatrix} -2 & -2+2i & -2+2i & 2i \\ -2-2i & 2 & -2 & 0 \\ -2-2i & -2 & 2 & 0 \\ -2i & 0 & 0 & 2 \end{pmatrix} \quad (24)$$

This matrix satisfies the constraint  $\text{Tr}(\rho) = 1$ , but with eigenvalues  $\lambda_1 = \frac{-2+2\sqrt{3}}{4}$ ,  $\lambda_2 = \frac{-2-2\sqrt{3}}{4} < 0$ ,  $\lambda_3 = \lambda_4 = 1$ . Since a *physical* matrix must be a positive operator [5], it cannot be regarded as representing a physical system. The same is true for other values of  $N$ .

In order to find a valid interval for  $N = 2$ , consider a particular example where all the coefficients are equal to some constant  $c_{\alpha_1, \dots, \alpha_N} = c$  in Eq.(23), and let us impose  $\lambda \geq 0$  for the eigenvalues of the resulting matrix. This leads to  $-0.15 \leq c \leq 0.33$ . It should be noted that this is only one possible set of values for the coefficients. Observe that the intervals  $-1 \leq c < -0.15$  and  $0.33 < c \leq 1$  define infinite non-physical matrices within  $-1 \leq c \leq 1$ .

With the new interval, the eigenvalues for the case  $N = 2$  and  $c = -0.15$ , are all positive and  $\rho$  satisfies  $\text{tr}(\rho) = 1$ :

$$\{\lambda_i\} = \{0.007596, 0.267404, 0.362499, 0.362500\}$$

The above considerations are in accordance with the so-called *entanglement fidelity*, a quantum measure for the degree of entanglement in a system [5]. Quantum noisy destroys entanglement leading the fidelity to its classical value [5]. To take noisy into account in our experiment, we notice that, within the time scale of the spin-spin (transverse) relaxation time,  $T_2$ , a NMR experiment can be formally viewed as a depolarization channel quantum process. In this noisy process, the initial density matrix  $\rho$  is replaced by the identity with probability  $p$ , or is left untouched with probability  $1 - p$  [5]:

$$\varepsilon(\rho) = p \frac{I_4}{4} + (1 - p)\rho$$

Comparing  $\varepsilon(\rho)$  with Eq. (22), one can identify  $p \equiv 1 - \varepsilon$ . Writing  $\varepsilon(\rho) = \sum_k E_k \rho E_k^\dagger$ , where  $E_k$  are the operation elements [5] for the depolarization channel which, in the case of two-qubits, are:

$$\begin{aligned}
 E_1 &= \sqrt{1 - \frac{15(1-\epsilon)}{16}} I_4, \quad E_2 = \sqrt{\frac{1-\epsilon}{16}} \sigma_1 \otimes \sigma_1, \quad E_3 = \sqrt{\frac{1-\epsilon}{16}} \sigma_1 \otimes \sigma_2 \\
 E_4 &= \sqrt{\frac{1-\epsilon}{16}} \sigma_1 \otimes \sigma_3, \quad E_5 = \sqrt{\frac{1-\epsilon}{16}} \sigma_2 \otimes \sigma_1, \quad E_6 = \sqrt{\frac{1-\epsilon}{16}} \sigma_2 \otimes \sigma_2 \\
 E_7 &= \sqrt{\frac{1-\epsilon}{16}} \sigma_2 \otimes \sigma_3, \quad E_8 = \sqrt{\frac{1-\epsilon}{16}} \sigma_3 \otimes \sigma_1, \quad E_9 = \sqrt{\frac{1-\epsilon}{16}} \sigma_3 \otimes \sigma_2 \\
 E_{10} &= \sqrt{\frac{1-\epsilon}{16}} \sigma_3 \otimes \sigma_3, \quad E_{11} = \sqrt{\frac{1-\epsilon}{16}} I_4 \otimes \sigma_1, \quad E_{12} = \sqrt{\frac{1-\epsilon}{16}} I_4 \otimes \sigma_2 \\
 E_{13} &= \sqrt{\frac{1-\epsilon}{16}} I_4 \otimes \sigma_3, \quad E_{14} = \sqrt{\frac{1-\epsilon}{16}} \sigma_1 \otimes I_4, \quad E_{15} = \sqrt{\frac{1-\epsilon}{16}} \sigma_2 \otimes I_4 \\
 E_{16} &= \sqrt{\frac{1-\epsilon}{16}} \sigma_3 \otimes I_4
 \end{aligned}$$

From this, we can calculate the entanglement fidelity [5],  $F = \sum_k |tr(\rho E_k)|^2$  which, for the limiting case  $c_{\alpha_1, \alpha_2} = -1$  results independent of  $\epsilon$ :

$$F = \sum_{k=1}^{16} |tr(\rho E_k)|^2 = \frac{1}{16}(1 + 15\epsilon) + 15 \frac{(1-\epsilon)}{16} = 1$$

This result shows that the limit  $c_{\alpha_1, \alpha_2} = -1$  for the Pauli expansion coefficients is not physically valid. On another hand, if we take  $c = -0.15$  we find, after working  $\rho_1$  and  $\rho_\epsilon$  out,

$$F(\epsilon) = 0.0836 + 0.9164\epsilon$$

which reaches the value for entanglement,  $F = 0.5$ , at  $\epsilon \approx 0.45$ , in agreement with our previous analysis.

Finally, if we take  $\rho_1$  as the cat state:

$$\rho_1 = \begin{pmatrix} 0.5 & 0 & 0 & 0.5 \\ 0 & 0 & 0 & 0 \\ 0 & 0 & 0 & 0 \\ 0.5 & 0 & 0 & 0.5 \end{pmatrix} \quad (25)$$

and calculate  $\rho_\epsilon$ , we find for the entanglement fidelity:

$$F(\epsilon) = 0.25 + 0.75\epsilon$$

which reaches 0.5 for  $\epsilon = 0.33$ . This value coincides with the upper bound given in [13].

The experimental characterization of entanglement is not simple, but one can seek for indirect evidences by looking at quantities which can be derived from density matrices, such as

the entropy. As it must be for any pure state, the entropy of an entangled state is zero. However, quite contrary to what happens to pure *product states*, the entropy of individual qubits of entangled states is maximum. Therefore, we can expect a decrease in the entropy of a two-partite system in an entangled state [5].

From tomographed density matrices one can build the entropy according to:

$$S_{A,B} = -\text{Tr}(\rho \ln \rho) \quad (26)$$

The entropy of individual qubits can be obtained from the partial trace operation [5]:

$$S_A = -\text{Tr}_A[\text{Tr}_B(\rho) \ln(\text{Tr}_B \rho)]; \quad S_B = -\text{Tr}_B[\text{Tr}_A(\rho) \ln(\text{Tr}_A \rho)] \quad (27)$$

where  $\text{Tr}_{A(B)}$  is the partial trace over the qubit  $A(B)$  Hilbert space [5]. Since the entropy is additive only for product states [5], that is  $S_{A,B} = S_A + S_B$ , the difference  $\Delta S \equiv |S_{A,B} - S_A - S_B|$  (is equal to the quantum mutual information, and according to [29] is also the total amount of correlations, for an arbitrary bipartite quantum state) should be (ideally) zero for product states and maximum for entangled states. The table below shows the calculated  $\Delta S$  from tomographed density matrices of various product states (computational base states and

Hadamard states) and two Bell states. One notice that  $\Delta S$  is clearly larger in the case of entangled states.

TABLE 1: Quantum states and their respective quantum mutual information, determined experimentally, as explained on the text.

State representation	$ \Delta S (\times 10^{-7})$
$\frac{1}{\sqrt{2}}[ 01\rangle +  10\rangle]$	0.87
$\frac{1}{\sqrt{2}}[ 01\rangle -  10\rangle]$	0.85
$ 00\rangle$	0.13
$ 01\rangle$	0.09
$ 10\rangle$	0.02
$ 11\rangle$	0.08
$\frac{1}{\sqrt{2}}[ 00\rangle +  01\rangle]$	0.28
$\frac{1}{\sqrt{2}}[ 00\rangle -  01\rangle]$	0.16
$\frac{1}{\sqrt{2}}[ 01\rangle +  11\rangle]$	0.35
$\frac{1}{\sqrt{2}}[ 01\rangle -  11\rangle]$	0.39

## VII. PERSPECTIVES FOR NMR QUANTUM COMPUTING

NMR has been, by far, the most successful technique in the demonstration of the principles of quantum computing in small systems, and was responsible for the initial excitement which led to a number of important results in quantum computation and quantum information. NMR has the optimal tools to implement quantum logic gates, but unfortunately the highly mixed states of bulk NMR samples, pose serious difficulties in what concerns the interpretation of experiments, particularly the characterization of entanglement. In view of this picture, one could ask: what is the future for NMR quantum computing? Recent important experimental advances suggest that there is reason to be optimistic!

First of all, it is important to realize that the discussion about producing or not entanglement in NMR quantum computing concerns the nature of the *sample*, and not the *working principles* of the technique. Besides, although important, entanglement is not always present in quantum computation algorithms, the best example being the Grover search algorithm [5]. There is no doubt that radiofrequency pulses implement the universal set of quantum logic gates, upon which quantum computers can be built. Therefore, if an appropriate sample could be produced, would NMR quantum chips become a reality? The answer is yes, they would. Important recent achievements [11] show that the problem of the exponentially small value of  $\epsilon$  can be suppressed using laser techniques to

pump the spins into a true pure state. Experiments have currently produced  $\epsilon \approx 0.9$ .

In what concerns a possible quantum chip architecture, the first concrete proposal was made in 1998 by Bruce Kane [30]. In his design, an array of phosphorus nuclei is embedded in a silicon lattice. Kane showed that if such an array could be built (the atoms should be only a few angstroms apart), the hyperfine interaction between neighbor nuclei could be controlled through electrical gates, and quantum logic gates implemented by conventional NMR. Since in this arrangement the array of phosphorus does not form a statistical ensemble, the design would not be subject to the difficulties pointed by Braunstein et. al. [13]. An interesting variation to this idea is the “all silicon NMR quantum computer” proposed by Ladd and co-workers [31].

Although important drawbacks on Kane’s design were pointed out by Koiller et al., [32], who also made innovative refinements to the original idea [33], his work brought the notion that advantages could be taken from the well known semiconductor technology into quantum computation, and various groups around the world pursue this idea.

Finally, one must mention that one of the main difficulties with Kane’s design and its variations, concerns the sensitivity of detection. The sensitivity of conventional NMR is restricted to a minimum of about  $10^{15}$  nuclear spins. In the original Kane’s proposal, the detection should be made on the electronic charge, rather than directly on the nuclear spins. In the Ref. [31] it is suggested that optical techniques would do well in preparing initial states, whereas read out operations could be performed using cyclic adiabatic inversion. Both difficulties (initial state preparation and readout) seem to be very close to be suppressed. First Anwar et al., [11] have shown how to prepare almost pure initial states using laser techniques. Second, Rugar et al., [12] combined the techniques of NMR and AMF (Atomic Force Microscopy) to a technique known as MRFM (Magnetic Resonance Force Microscopy) to produce NMR tomographic images with resolution of a single spin! This is very encouraging, since it means the possibility of manipulating individual qubits on a quantum chip, bringing new perspectives into the original idea of Kane. The development in this area follows closely the fast growing field of nanotechnology, and important advances can be expected for the next few years. In conclusion, the general picture is very encouraging and points to a rapid progress in both, architecting quantum chips, manipulation of individual qubits, and increasing the detection sensitivity. These are the very basic ingredients towards a large scale quantum computer.

- 
- [1] Alexander G. Stepanov, Russian Chemical Reviews, 563 (1999).  
 [2] A.G. Palmer, Current Opinion in Biotechnology, 4, 385 (1993)  
 [3] Ae Ran Lim and Se-Young Jeong, J. Phys.: Condens. Matter 10, 9841 (1998).  
 [4] K.V.Chary, H.S. Atreya, Journal of Postgraduate Medicine, 48,

- 1 (2002).  
 [5] M.A. Nielsen and I.L. Chuang, *Quantum computation and Quantum information*, Cambridge University Press. Cambridge (2002).  
 [6] N.A. Gershenfeld and I.L. Chuang, 275, 350 (1997).  
 [7] D.G. Cory, A.F. Fahmy, and T.F. Havel, Proc. Natl. Acad. Sci.



- USA, **94**, 1634 (1997).
- [8] D.G. Cory, M. Price, W. Maas, E. Knill, R. Laflamme, W.H. Zurek, T.F. Havel, and S.S. Samaroo, Phys. Rev. Lett. **81**, 2152 (1998).
- [9] J.A. Jones, M. Mosca, and R.H. Hansen, Nature, **393**, 344-346 (1998); S. Samaroo, C.H. Tseng, T.F. Havel, R. Laflamme, and D.G. Cory, Phys. Rev. Lett. **82**, 5381 (1999).
- [10] L.M.K. Vandersypen, M. Steffen, G. Breyta, C.S. Yannoni, R. Cleve, and I.L. Chuang, Phys. Rev. Lett. **85**, 5452 (2000); Y.S. Weinstein, M.A. Pravia, E.M. Fortunato, S. Lloyd, and D.G. Cory, Phys. Rev. Lett. **86**, 1889 (2001).
- [11] M.S. Anwar, D. Blazina, H.A. Carteret, S.B. Duckett, T.K. Halstead, J.A. Jones, C.M. Kozak, and R.J.K. Taylor, Phys. Rev. Lett. **93**, 040501 (2004).
- [12] D. Rugar, R. Budakian, H.J. Mamin, and B.W. Chui, Letters to Nature, **430**, 329 (2004).
- [13] S.L. Braunstein, C.M. Caves, R. Jozsa, N. Linden, S. Popescu, and R. Schack, Phys. Rev. Lett. **83**, 1054 (1999).
- [14] J.D. Bulnes, R.S. Sarthour, E.R. de Azevedo, F.A. Bonk, J. C. C. Freitas, A.P. Guimarães, T.J. Bonagamba, and I.S. Oliveira, (quant-ph/0404020).
- [15] A. Peres, *Quantum Theory: Concepts and Methods* (Kluwer, Dordrecht, The Netherlands, 1993).
- [16] A. O. Barut, and M. Bozic, Il Nuovo Cimento, **101** B (5), 595 (1988).
- [17] L.M.K. Vandersypen, M. Steffen, G. Breyta, C.S. Yannoni, R. Cleve, and I.L. Chuang, Nature **414**, (6866), 883 (2001).
- [18] M.A. Nielsen, E. Knill, and R. Laflamme, Nature **396**, 52 (1998).
- [19] M. Mehring, J. Mende, and W. Scherer, Phys. Rev. Lett. **90**, 153001 (2003).
- [20] C.P. Slichter, *Principles of Magnetic Resonance* (Springer-Verlag, Berlin, 1990).
- [21] A. Peres, Phys. Rev. Lett. **77** (8), 1413 (1996); M. Horodecki, P. Horodecki, R. Horodecki, Phys. Lett. A **223** (1-2): 1 (1996).
- [22] A.K. Khitrin and B.M. Fung, J. Chem. Phys. **112**, 6963 (2000).
- [23] N. Sinha, T.S. Mahesh, K.V. Ramanathan, and A. Kumar, J. Chem. Phys. **114**, 4415 (2001).
- [24] K. Vogel and H. Risken, Phys. Rev. A **40**, 7113 (1989); A.M. Childs, I.L. Chuang, and D.W. Leung, Phys. Rev. A **64**, 012314 (2001).
- [25] F.A. Bonk, R.S. Sarthour, E.R. de Azevedo, J.D. Bulnes, J.C.C. Freitas, T.J. Bonagamba, A.P. Guimarães, and I.S. Oliveira, Phys. Rev. A **69**, 042322 (2004); F.A. Bonk, E.R. de Azevedo, R.S. Sarthour, J.D. Bulnes, J.C.C. Freitas, A.P. Guimarães, I.S. Oliveira, and T.J. Bonagamba, J. Mag. Res. **175**, 226 (2005).
- [26] R.S. Sarthour, E.R. de Azevedo, F.A. Bonk, E.L.G. Vidoto, T.J. Bonagamba, A.P. Guimarães, J. C. C. Freitas, and I.S. Oliveira, Phys. Rev. A **68**, 022311 (2003).
- [27] A. Ghosh and A. Kumar, J. Mag. Res. **173**, 125 (2005).
- [28] G.L. Long, H.Y. Yan, Y.S. Li, C.C. Tu, S.J. Zhu, D. Ruan, Y.Sun, J.X. Tao, and H.M. Chen, Theor. Phys. **38**, 306 (2002); G.L. Long, Y.F. Zhou, J.Q. Jin, and Y. Sun, arXiv: quant-ph/0408079, (2004).
- [29] B. Groisman, S. Popescu and A. Winter, quant-ph/0410091.
- [30] B.E. Kane, Nature **393**, 133 (1998).
- [31] T.D. Ladd, J.R. Goldman, F. Yamaguchi, Y. Yamamoto, E. Abe, and K.M. Itoh, All-Silicon Quantum Computer, Phys. Rev. Lett. **89**, 017901 (2002).
- [32] B. Koiller, X.D. Hu, and S. Das Sarma, Phys. Rev. Lett. **88**, 027903 (2002).
- [33] B. Koiller, X.D. Hu, and S. Das Sarma, Phys. Rev. B **66**, 115201 (2002).